Communications

Photoinduced Hydrogen Evolution Using Bipyridinium Salts as Electron Carrier

Sir:

Photochemical redox systems have been proposed for solar energy utilization.[1,2] The systems as illustrated in Scheme I, including a photosensitizer (S), an electron donor (D), and an electron carrier (C), have been able to evolve hydrogen from water when a suitable catalyst can be applied. In the course of our studies,[3,4] we found that zinc *meso*-tris(sulfonatophenyl)porphyrin ($Zn(TPPS_3)$) exhibits particularly high activity as a photosensitizer for the photoredox reaction in the system. The electron carrier employed almost exclusively in these studies is methylviologen except for a few cases.[5,6] It is desirable to explore other suitable electron carriers.

In this paper we describe some bipyridinium salts that are more suitable electron carriers than methylviologen. To clarify why hydrogen evolution rates are so high when some bipyridinium salts are used as electron carriers, kinetic studies were carried out by laser flash photolysis.

Experimental Section. The bipyridinium compounds used as electron carriers are shown in Figure 1. The compounds A, B, C, and D were synthesized according to the literature.[7,8] The sample solution, which consisted of $Zn(TPPS_3)$, electron carrier, 2-mercaptoethanol (RSH) as an electron donor, and hydrogenase as a catalyst in phosphate buffer (pH 7.0), was deaerated by repeated freeze–pump–thaw cycles. A typical experiment was performed under anaerobic reaction conditions as follows: to 2.03 $\times 10^{-7}$ mol·dm^{-3} of $Zn(TPPS_3)$, 0.197 mol·dm^{-3} of RSH, and 1.27 $\times 10^{-4}$ mol·dm^{-3} of bipyridinium compound in water was added the hydrogenase. In these experiments an excess amount of hydrogenase was used to make the photoreduction of electron carriers the rate-determining step of the hydrogen evolution. The volume of the reaction mixture was adjusted to 6.5 mL with 0.02 mol·dm^{-3} phosphate buffer (pH 7.0). In the photolysis with continuous irradiation, the sample in a Pyrex cell equipped with a magnetic stirrer was irradiated with light from a 200-W tungsten lamp. Light of wavelength less than 390 nm was cut off by a Toshiba L-39 filter.

Conventional laser photolysis was carried out by using a Nd-YAG laser, Model HY-500 from JK Lasers Ltd., equipped with
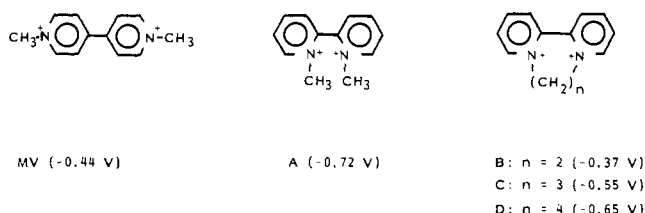

Figure 1. Electron carriers. (Values in parentheses indicate the redox potentials vs. NHE.)
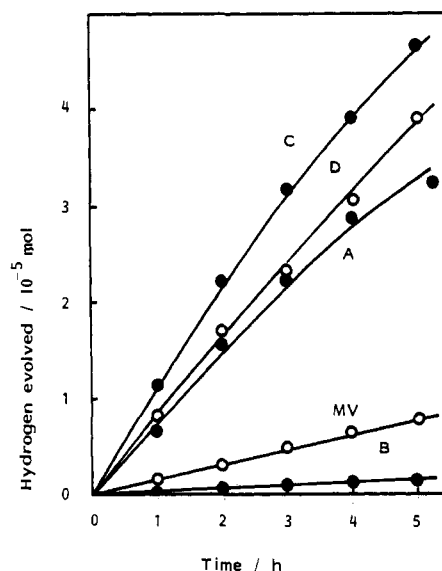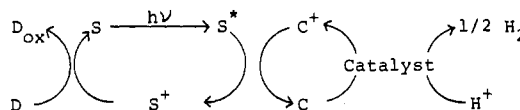

Time / h

Figure 2. Time dependence of hydrogen evolution for a sample solution containing RSH (0.2 mol·dm^{-3}), $Zn(TPPS_3)$ (7.03 $\times 10^{-7}$ mol·dm^{-3}), bipyridinium salt (1.27 $\times 10^{-4}$ mol·dm^{-3}), and hydrogenase (0.5 mL) irradiated by visible light at 30 °C.

Scheme I

the second, third, and fourth harmonic generators. The second harmonic (532 nm), ca. 100 mJ·cm^{-2} with flash duration of 20 nm, was used for excitation of the sample solutions throughout this study. Analyzing light beams from a xenon lamp (Ushio UXL-150 D, 150 W) were intensified by a factor of ca. 20 during the detection of the transient spectra. Transient spectra having lifetimes longer than 200 μs were measured without intensification of the analyzing light beams. The light beam, after passage through a sample cell, came into the extrance slit of a monochromator (Model MC-20 N from Ritsu Applied Optical Co.).

(1) Darwent, J. R.; Douglas, P.; Harriman, A.; Porter, G.; Richoux, M.-C. *Coord. Chem. Rev.* **1982**, *44*, 83 and references therein.
(2) Kiwi, J.; Kalyanasundaram, K.; Gratzel, M. *Struct. Bonding (Berlin)* **1982**, *49*, 37 and references therein.
(3) Okura, I.; Takeuchi, M.; Kim-Thuan, N. *Chem. Lett.* **1980**, 765.
(4) Okura, I.; Takeuchi, M.; Kim-Thaun, N. *Photochem. Photobiol.* **1981**, *33*, 413.
(5) Johansen, O.; Launikonis, A.; Loder, J. W.; Mau, A. W. H.; Sasse, W. H. F.; Swift, J. D.; Wells, D. *Aust. J. Chem.* **1981**, *34*, 981.
(6) Amouyal, E.; Zidler, B. *Isr. J. Chem.* **1982**, *22*, 117.
(7) Schmalzl, K. J.; Summers, L. A. *Aust. J. Chem.* **1977**, *30*, 657.
(8) Homer, R. F.; Tolinson, T. E. *J. Chem. Soc.* **1960**, 2498.

Table I. Kinetic Parameters Obtained from Laser Flash Photolysis

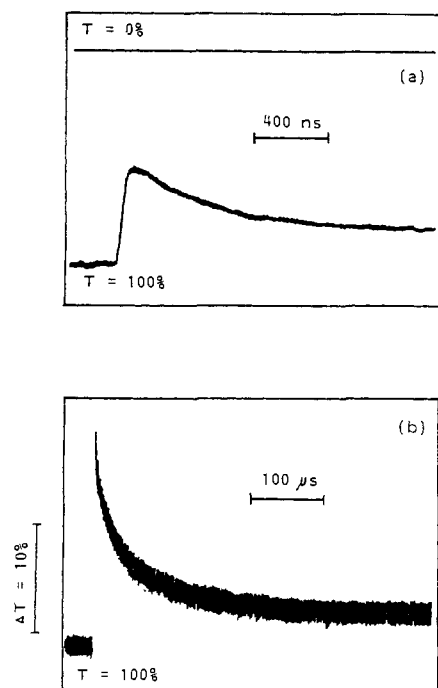|	MV	A	B	C	D
$k_q/\text{mol}^{-1}\cdot\text{dm}^3\cdot\text{s}^{-1}$	$(1.5 \pm 0.3) \times 10^{10}$	$(2.5 \pm 1.8) \times 10^9$	$(9.9 \pm 0.9) \times 10^9$	$(8.7 \pm 1.3) \times 10^9$	$(5.3 \pm 1.2) \times 10^9$
k_b (relative values)	100	21	38	18	17

Figure 3. Oscilloscopic photographs obtained from laser flash photolysis of an aqueous solution of $Zn(TPPS_3)$ (3.03×10^{-5} mol·dm^{-3}) containing compound C (2.50×10^{-4} mol·dm^{-3}). The time scale is different in part a and part b.
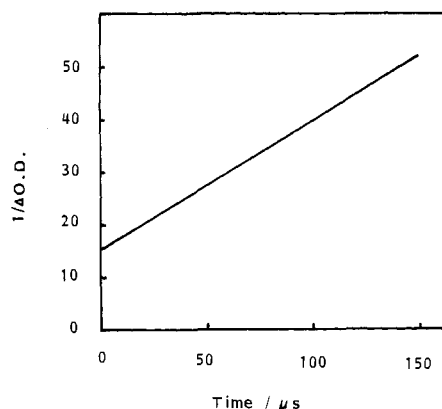

Figure 4. Second-order plot (OD^{-1} vs. t) based on the data shown in Figure 3b.

The output from a Hamamatsu photomultiplier (R 758) attached to the exit slit of the monochromator was displayed on a Tektronix oscilloscope, Model 7904.

Results and Discussion. When an aqueous solution containing RSH, $Zn(TPPS_3)$, bipyridinium salt, and hydrogenase was irradiated, hydrogen evolution with a stationary rate was observed as shown in Figure 2. It is evident that all the compounds shown in Figure 1 can serve as electron carriers for photoinduced hydrogen evolution. Hydrogen evolution rates of the systems for electron carriers A, C, and D were much greater than that for methylviologen.

Under the reaction conditions where the rate-determining step of hydrogen evolution is the step of the photoreduction of electron carriers, the bipyridinium salts with low redox potentials will be favorably photoreduced. The order of the rate values, however, does not always coincide with the order of the redox potentials of the bipyridinium salts. The rate difference may depend on the

efficiency of ion separation of electron transfer from the photoexcited $Zn(TPPS_3)$ to the bipyridinium salt, or it may depend on the difference between the association constants of $Zn(TPPS_3)$ and the bipyridinium salts. The complexes between $Zn(TPPS_3)$ and the viologens such as methylviologen do not take part in the photoreduction of the viologens, and only uncomplexed $Zn(TPPS_3)$ plays an important role in the reaction.[9-12] Under the reaction conditions, however, the greatest part of $Zn(TPPS_3)$ is in the uncomplexed form. To clarify why the rates strongly depend on the molecular structure of bipyridinium salts, the rate constants of both the following quenching reaction (eq 1) and the back-reaction (eq 2) are determined by laser flash photolysis, where

$$Zn(TPPS_3)^* + V^{2+} \rightarrow Zn(TPPS_3)^+ + V^+ \quad (1)$$

$$Zn(TPPS_3)^+ + V^+ \rightarrow Zn(TPPS_3) + V^{2+} \quad (2)$$
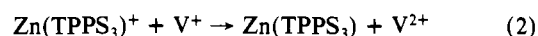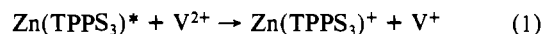
$Zn(TPPS_3)^*$ and $Zn(TPPS_3)^+$ are the photoexcited and oxidized forms of $Zn(TPPS_3)$, respectively, and V^{2+} and V^+ denote oxidized and reduced forms of bipyridinium salts, respectively.

As reported previously,[13] the triplet state of $Zn(TPPS_3)$ has markedly long lifetimes, such as 1.6 ms. In the presence of a bipyridinium salt, the decay rate of the transient spectrum at λ_{max} = 470 nm (the peak wavelength of the T–T absorption band due to triplet $Zn(TPPS_3)$) increased. In a short period less than 10 μs after a laser flash, the decay tendency follows first-order kinetics (typical oscilloscope traces in the case of compound C are shown in Figure 3). From the relation between lifetimes and various concentrations of bipyridinium salts are determined the quenching rate constants as shown in Table I. These values are close to that for the diffusion-controlled process.

In the longer periods of more than 10 μs, the decay of the transient spectrum with λ_{max} = 470 nm follows second-order kinetics. A typical oscilloscope trace and the second-order plot of the curve are shown in Figure 3b and Figure 4. From the second-order plot (linear plot, OD^{-1} vs. t), the relative back-reaction rate constants (k_b) were determined as shown in Table I. The quenching efficiency of $^3Zn(TPPS_3)^*$ by V^{2+} is expressed as $k_q[V^{2+}]/(k' + k_q[V^{2+}])$, where k_q is the rate constant for quenching by V^{2+}. As shown in Table I, k_q values are close to those for the diffusion-controlled process, and $k_q[V^{2+}] \gg k'$ (6.2×10^2 s^{-1}). So, the quenching efficiency of $^3Zn(TPPS_3)$ by V^{2+} is almost unity and does not depend on the types of bipyridinium salts. On the other hand, k_b values strongly depend on them. When the bipyridinium salts showing the smaller k_b values are used, the higher hydrogen evolution rates were observed. As compound B does not have enough redox potential to reduce protons to evolve hydrogen, the hydrogen evolution rate is very low, though the k_b value is relatively small. From the above results, it is apparent that the back-reaction (recombination reaction) takes part in the photoinduced hydrogen evolution reaction in these systems.

(9) Rougee, M.; Ebbesen, T.; Ghetti, F.; Bensasson, R. V. *J. Phys. Chem.* **1982**, *86*, 4404.
(10) Okura, I.; Kusunoki, S.; Aono, S. *Inorg. Chim. Acta* **1983**, *77*, L99.
(11) Okura, I.; Kusunoki, S.; Aono, S. *Inorg. Chem.* **1983**, *22*, 3828.
(12) Okura, I.; Kusunoki, S.; Aono, S. *Bull. Chem. Soc. Jpn.* **1984**, *57*, 1184.
(13) Okura, I.; Aono, S. *Inorg. Chim. Acta* **1984**, *86*, L55.

Department of Chemical Engineering   **Ichiro Okura***
Tokyo Institute of Technology   **Naruhiko Kaji**
Meguro-ku, Tokyo 152, Japan   **Shigetoshi Aono**
    Tatsuya Kita

The Institute of Physical and Chemical   **Akira Yamada**
    Research
Hirosawa, Wako-shi, Saitama 351, Japan

Received September 24, 1984

Structural Diversity of Homoleptic Ethane-1,2-dithiolato Complexes of the First Transition Series

Sir:

The current rapid development of transition-metal thiolate chemistry has been stimulated primarily by the discovery of a diversity of structural types with variant nuclearity[1–4] and the utility of certain complexes as precursors to new clusters and cages.[5–7] Despite these advances, the types and structural patterns of homoleptic thiolate complexes of first transition series elements in their common oxidation states have not been fully derived. The present results, in conjunction with previous information,[2a,b,3,4] provide a close approach to this objective by utilizing as the common ligand ethane-1,2-dithiolate, whose strong binding leads to homoleptic species. Because previous complexes of this ligand have the 2:1 $(S_2C_2H_4)^{2-}:M^{II,III}$ ratio, this ratio was employed in the new reaction systems, which are considered in order of increasing atomic number of the metal component. All reactions and manipulations were performed at ambient temperature under a pure dinitrogen atmosphere. Structures of reaction products are shown in Figure 1.

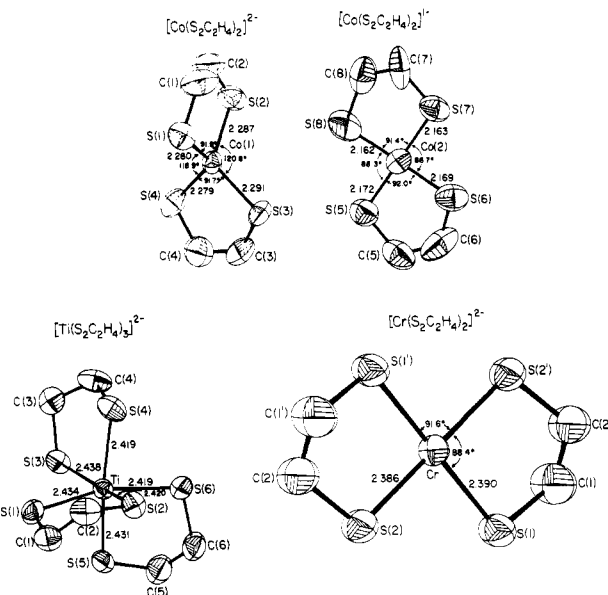The 2:1:1 $Na_2(S_2C_2H_4):TiCl_3:Et_4NBr$[8] reaction system in 50

Figure 1. Structures of $[Ti(S_2C_2H_4)_3]^{2-}$, $[Co(S_2C_2H_4)_2]^{2-}$, $[Co(S_2C_2H_4)_2]^-$, and $[Cr(S_2C_2H_4)_2]^{2-}$, showing 50% probability ellipsoids, atom-labeling schemes, and selected bond angles and distances.

mL of acetonitrile—after 2 days of stirring and addition of ether to the cold concentrated filtrate—afforded orange diamagnetic $(Et_4N)_2[Ti(S_2C_2H_4)_3]$.[9a] With this stoichiometry established, the compound (45%) was prepared more rationally in the 3:1:2 $Na_2(S_2C_2H_4):TiCl_4:Et_4NBr$ system in acetonitrile after similar workup and recrystallization from acetonitrile/ether. Despite the reaction ratio and anaerobic conditions, the (isolable) product is a tris-chelate Ti(IV) complex. The oxidation state is an apparent consequence of the extreme oxidative instability of the Ti(III) species ($E_{p,c}$ = −2.0 V vs. SCE, acetonitrile). $(Et_4N)_2[Ti-(S_2C_2H_4)_3]$ crystallizes in orthorhombic space group $Pna2_1$ with a = 21.151 (4) Å, b = 9.671 (1) Å, c = 15.046 (3) Å, and Z = 4.[10a] The anion structure approaches C_3 symmetry, as evident from these ranges of angles related under this symmetry, with one member of a set specified: S(1)–Ti–S(2), 3 at 82.8 (1)–82.9 (1)°; S(1)–Ti–S(3), 6 at 85.8 (1)–89.1 (1)°; S(1)–Ti–S(4), 3 at 105.1 (1)–108.3 (1)°; S(1)–Ti–S(6), 3 at 161.2 (1)–164.7 (1)°. Distances similarly divide into the sets Ti–S(1,3,5) and Ti–S(2,4,6) with mean values of 2.434 (4) and 2.419 (1) Å. The two S_3 planes are nearly parallel (dihedral angle 1.8°), and the projected twist angles ϕ = 35–42° indicate substantial distortion from octahedral (ϕ = 60°) toward trigonal-prismatic (ϕ = 0°) stereochemistry.

The 2:1:2 $Na_2(S_2C_2H_4):CrCl_2:Et_4NCl$[8] reaction system in 100 mL of acetonitrile—after $2^1/_2$ days of stirring and workup similar to that of the Ti system—gave violet, highly air-sensitive $(Et_4N)_2[Cr(S_2C_2H_4)_2]$[9b] (45%) upon recrystallization from acetonitrile/ether. The compound occurs in monoclinic space group $C2/c$ with a = 13.023 (2) Å, b = 17.369 (3) Å, c = 12.825 (2) Å, β = 103.97 (1)°, and Z = 4.[10b] Mononuclear $[Cr(S_2C_2H_4)_2]^{2-}$

(1) (a) Lane, R. W.; Ibers, J. A.; Frankel, R. B.; Papaefthymiou, G. C.; Holm, R. H. *J. Am. Chem. Soc.* **1977**, *99*, 84. (b) Dance, I. G. *J. Am. Chem. Soc.* **1979**, *101*, 6264. (c) Hagen, K. S.; Holm, R. H. *J. Am. Chem. Soc.* **1982**, *104*, 5496. (d) Hagen, K. S.; Holm, R. H. *Inorg. Chem.* **1984**, *23*, 418. (e) Henkel, G.; Tremel, W.; Krebs, B. *Angew. Chem., Int. Ed. Engl.* **1983**, *22*, 319. (f) Gaete, W.; Ros, J.; Solans, X.; Font-Altaba, M.; Briansó, J. L. *Inorg. Chem.* **1984**, *23*, 39. (g) Lacella, S.; Stevens, W. C.; Kurtz, D. M., Jr.; Richardson, J. W., Jr.; Jacobson, R. A. *Ibid.* **1984**, *23*, 930. (h) Tremel, W.; Krebs, B.; Henkel, G. *Angew. Chem., Int. Ed. Engl.* **1984**, *23*, 634. (i) Watson, A. D.; Rao, C. P.; Dorfman, J. R.; Holm, R. H. submitted for publication in *Inorg. Chem.* These references describe selected M(II)–thiolate structures.

(2) (a) Snow, M. R.; Ibers, J. A. *Inorg. Chem.* **1973**, *12*, 249. (b) Herskovitz, T.; DePamphilis, B. V.; Gillum, W. O.; Holm, R. H. *Ibid.* **1975**, *14*, 1426. (c) Millar, M.; Lee, J. F.; Koch, S. A.; Fikar, R. *Ibid.* **1982**, *21*, 4105. (d) Koch, S. A.; Maelia, L. E.; Millar, M. *J. Am. Chem. Soc.* **1983**, *105*, 5944.

(3) (a) Costa, T.; Dorfman, J. R.; Hagen, K. S.; Holm, R. H. *Inorg. Chem.* **1983**, *22*, 4091. (b) Christou, G.; Huffman, J. C. *J. Chem. Soc., Chem. Commun.* **1983**, 558.

(4) (a) Dorfman, J. R.; Holm, R. H. *Inorg. Chem.* **1983**, *22*, 3179. (b) Szeymies, D.; Krebs, B.; Henkel, G. *Angew. Chem., Int. Ed. Engl.* **1983**, *22*, 885; *Angew. Chem. Suppl.* **1983**, 1176. (c) Wiggins, R. W.; Huffman, J. C.; Christou, G. *J. Chem. Soc., Chem. Commun.* **1983**, 1313.

(5) (a) Hagen, K. S.; Reynolds, J. G.; Holm, R. H. *J. Am. Chem. Soc.* **1981**, *103*, 4054. (b) Coucouvanis, D.; Kanatzidis, M.; Simhon, E.; Baenziger, N. C. *J. Am. Chem. Soc.* **1982**, *104*, 1874.

(6) (a) Christou, G.; Hagen, K. S.; Holm, R. H. *J. Am. Chem. Soc.* **1982**, *104*, 1744. (b) Christou, G.; Hagen, K. S.; Bashkin, J. K.; Holm, R. H. *Inorg. Chem.*, in press.

(7) (a) Choy, A.; Craig, D.; Dance, I.; Scudder, M. *J. Chem. Soc., Chem. Commun.* **1982**, 1246. (b) Dance, I. G.; Choy, A.; Scudder, M. L. *J. Am. Chem. Soc.* **1984**, *106*, 6285.

(8) Molar ratios are given. The scale of each reaction is provided by the following quantities (mmol): TiCl₃, 5.0; TiCl₄, 5.0; CrCl₂, 10; CrCl₃·6H₂O, 12; CoCl₂, 34; NiCl₂·6H₂O, 57. All new compounds gave highly satisfactory total elemental analyses.

(9) Absorption spectra, λ_{max}, nm (ϵ_M): (a) $(Et_4N)_2[Ti(S_2C_2H_4)_3]$ (acetonitrile) 230 (38 900), 276 (sh, 8480), 355 (9810), 414 (10 400), 476 (sh, 4570); (b) $(Et_4N)_2[Cr(S_2C_2H_4)_2]$ (DMF) 556 (67), 620 (sh, 52); (c) $(Me_4N)_n[Cr_n(S_2C_2H_4)_{2n}]$ (Me₂SO) 296 (16 000), 500 (400), 560 (340), 660 (260) (calculated for n = 2); (d) $(Me_4N)_3[Co_2(S_2C_2H_4)_4]$ (acetonitrile) 316 (15 200), 360 (8050), 417 (5070), ~500 (sh, 580), 676 (2920), 708 (sh, 1900), 970 (200), 1200 (180); (e) $(n\text{-}Bu_4N)_2[Ni_2(S_2C_2H_4)_3]$ (acetonitrile) 448 (900), 592 (400).

(10) Data were collected at ambient temperature on a Nicolet R3m or P3F diffractometer with graphite-monochromatized Mo Kα radiation. Empirical absorption corrections were applied. Structures were solved by a combination of direct methods and subsequent difference Fourier maps followed by full-matrix least-squares refinement. Calculations were performed with use of SHELXTL programs: (a) $(Et_4N)_2[Ti(S_2C_2H_4)_3]$, 1865 unique data ($F_o^2 > 2.0\sigma(F_o^2)$), $R(R_w)$ = 3.4 (3.4)%; (b) $(Et_4N)_2[Cr(S_2C_2H_4)_2]$, 1631 unique data ($F_o^2 > 3\sigma(F_o^2)$), $R(R_w)$ = 4.5 (6.0)%; (c) $(Me_4N)_3[Co_2(S_2C_2H_4)_4]$, 1695 unique data ($I > 2.5\sigma(I)$), $R(R_w)$ = 5.4 (5.3)%.